Available online at www.sciencedirect.com

ScienceDirect

Energy Procedia 40 (2013) 77 – 86

Energy Procedia

European Geosciences Union General Assembly 2013, EGU

\Division Energy, Resources & the Environment, ERE

# Wind effect on PV module temperature: Analysis of different techniques for an accurate estimation

C. Schwingshackl[a,*], M. Petitta[a,b], J.E. Wagner[a], G. Belluardo[c], D. Moser[c], M. Castelli[a,d], M. Zebisch[a] and A. Tetzlaff [a]

[a] *EURAC Research, Institute for Applied Remote Sensing, Viale Druso 1, 39100 Bolzano, Italy*
[b] *ENEA, Via Anguillarese 301, 00123 Roma, Italy*
[c] *EURAC Research, Institute for Renewable Energy, Viale Druso 1, 39100 Bolzano, Italy*
[d] *DICA, University of Trento, Italy*

**Abstract**

Photovoltaic (PV) module temperature predictions are crucial to accurately assess the efficiency of PV installations. In this study we focus on the cooling effect of wind on PV cell temperature. We show that for most of the technologies installed at a PV test facility in Bolzano (Italy), models including wind data predict PV cell temperature better than standard approaches which do not include wind data. Moreover, we show that wind data from numerical weather prediction models can replace in-situ wind measurements: when they are used as model input, the prediction also improves significantly compared to the standard approach.



*Keywords:* Photovoltaic module; Module temperature; Temperature estimation; Solar cell; Nominal operating cell temperature; PV cell operating temperature;

## 1. Introduction

As the photovoltaic industry grows, there is an increasing demand for high quality energy yield predictions. There are several factors affecting the energy yield. The most important is the incident

* Corresponding author. Tel.: +49-6221-54-6334; fax: +49-6221-54-6405.
*E-mail address:* clemens.schwingshackl@iup.uni-heidelberg.de


doi:10.1016/j.egypro.2013.08.010

**Nomenclature**

| | |
|---|---|
| $h_w$ | wind convection coefficient |
| $I$ | irradiance |
| $T_a$ | ambient temperature |
| $T_c$ | cell/module temperature |
| $U_0, U_1$ | Faimann coefficients, Koehl et al. [6] |
| $U_{PV}$ | heat exchange coefficient, Mattei et al. [2] |
| $v$ | wind speed |
| $v_f$ | wind speed measured 10 meters above the ground |
| $v_w$ | local wind speed close to the module |
| ECMWF | European Centre for Medium range Weather Forecast |
| NWP | Numerical Weather Prediction |

*Greek symbols*

| | |
|---|---|
| $\alpha$ | absorption coefficient of the solar cells |
| $\beta$ | temperature coefficient of maximal power of the solar cells |
| $\eta$ | efficiency of the solar cells |
| $\tau$ | transmittance of the cover system |

*Subscripts*

| | |
|---|---|
| a | ambient |
| c | cell/module |
| NOCT | nominal operating cell temperature |
| STC | standard test conditions |

solar irradiance on the module plane. However, since solar cells are semi-conductors, they are also very sensitive to temperature. The characteristic power curve is affected significantly by the module temperature. The open-circuit voltage decreases significantly with increasing PV module temperature (values are up to -0.45 %/K for crystalline silicon) whereas the short circuit current increases only slightly (values range between 0.04 and 0.09 %/K) [1]. The solar cell efficiency is usually measured under standard test conditions (STC), with PV cell temperature of 25 °C, irradiance of 1000 W/m$^2$ and air mass $AM = 1.5$. These conditions are rarely met at outdoor installations. The PV cell temperature, which can be assumed to be the same as the temperature of the PV module [2], shows large variability under outdoor conditions. It has therefore an important impact on the solar cell efficiency and thus, on the energy yield. On a cloud free summer day in Central Europe, the cell temperature can easily reach 60 °C for free standing systems. This leads to a considerable reduced energy yield. King et al. [3] analysed three different PV technologies and found that the energy yield is lowered by 2 to 10 % at high module temperatures. Accurate cell temperature predictions are thus a key factor to better assess the efficiency of PV installations.

For most PV installations direct measurements of the cell temperature are not available. Hence, it is desirable to parameterize the physical relation between the PV cell temperature, incoming irradiance and relevant meteorological parameters, such as wind, which is the most important factor influencing the cell temperature. The commonly used standard approach to model the cell temperature is based on ambient air temperature and in-plane irradiance measurements alone and does not include the influence of wind on the cell temperature [4].

In our study we focus on the cooling effect of wind on the PV cell temperature. Various authors (e.g. Skoplaki et al. [5], Koehl et al. [6], Mattei et al. [2], Kurtz et al. [7]) suggest different approaches to include the wind effect in PV cell temperature estimations. Koehl et al. [6] report a wind cooling effect of 15-20 °C for wind speeds of 10 m/s at solar irradiance of about 1000 W/m$^2$.

In former studies (e.g. [2], [5], [6], [7]) the different models were tested and validated using in-situ wind data, measured directly at or nearby the PV test sites. However, in-situ wind measurements are rare and it is thus necessary to replace those data with wind data from numerical weather prediction (NWP) models. In this study, we compare the performance of different approaches to estimate the PV cell temperature and for the first time we analyse model performances using wind data from the European Centre for Medium range Weather Forecast (ECMWF) model.

For our analysis we used data from a large PV power plant located in the alpine city Bolzano, Italy. This PV field includes different PV technologies and is equipped with several instruments to monitor solar radiation, ambient and cell temperature as well as wind speed [8]. First, we compared modelled and measured PV cell temperatures for different approaches using in-situ wind data. Later, we replaced the in-situ wind measurements with wind data from the ECMWF model and compared the model performance with the previous analysis.

Our results show that the inclusion of wind plays an important role for PV cell temperature estimations and that numerical weather prediction data can be used to replace in-situ wind measurements for locations where in-situ wind data are missing.

## 2. Methods

### *2.1. Data*

In-situ measurements from our multi-technology photovoltaic test-facility at the Airport Bolzano Dolomiti (ABD) were used to analyse wind cooling effects on PV cell temperatures. This test-facility is located at the bottom of an alpine valley in Bolzano, Italy (46° 27' 28'' N, 11° 19' 43'' E, 247 meters above sea level) and is described in detail by Belluardo et al. [8].

The PV cell temperatures of five different photovoltaic technologies were evaluated for one entire year, from March 2011 to February 2012. To avoid disturbing influences of fast irradiance changes at sunrise and sunset, we only analysed data from 10 a.m. to 3 p.m. The five monitored modules are based on monocrystalline silicon (m-Si), polycrystalline silicon (p-Si), amorphous silicon (a-Si), microcrystalline silicon (μc-Si) and cadmium telluride (CdTe). The characteristics of the investigated PV technologies are shown in table 1.

Table 1. Characteristics of investigated PV technologies

| PV technology | Monocrystalline silicon (m-Si) | Polycrystalline silicon (p-Si) | Amorphous silicon (a-Si) | Microcrystallin e silicon (μc-Si) | Cadmium telluride (CdTe) |
|---|---|---|---|---|---|
| Type | glass-polymer | glass-polymer | glass-glass | glass-polymer | glass-glass |
| NOCT (°C) | 45 | 46 | 46 | 44 | 45 |
| Module efficiency $\eta_{STC}$ (%) | 18.4 | 14.1 | 6.0 | 9.5 | 10.7 |
| Temperature coefficient of maximal power $\beta_{STC}$ (%/K) | -0.38 | -0.45 | -0.19 | -0.24 | -0.25 |
| $U_0$ (specified by Koehl et al. [6]) | 30.02 | 30.02 | 25.73 | 30.02 | 23.37 |
| $U_1$ (specified by Koehl et al. [6]) | 6.28 | 6.28 | 10.67 | 6.28 | 5.44 |

The investigated modules are mounted on fixed racks with a 30° tilt angle and an orientation of 8.5° west of south. The PV cell temperature is recorded at the back of the modules using Pt100 sensors. The meteorological parameters including in-plane irradiance, ambient temperature, wind speed and wind direction are measured through sensors installed at a weather station placed next to the PV plant. In-plane irradiance is measured using thermopile-based pyranometer (CMP11), ambient temperature is recorded two meters above ground and wind speed is registered using a two-axis ultrasonic anemometer installed 2.5 meters above the ground (0.5 meters above the PV modules). All in-situ measurements are performed with a frequency of 1 minute and averaged on 15-minutes time intervals.

In the second part of our analysis we replaced the in-situ wind measurements with wind data from ECMWF and calculated again the PV cell temperatures. We used ECMWF 10 m analysis wind fields which are available every 6 hours at 00, 06, 12 and 18 UTC at a 0.125° x 0.125° grid resolution. We have extracted the u (west-east wind component) and v (south-north wind component) wind components from the lowest model level (10 m above ground) for the model grid point closest to the airport of Bolzano (46° 30' N, 11° 18' E). We computed the ECMWF 10-m height wind speed $v_{ECMWF}$ from the wind components $u$ and $v$: $v_{ECMWF} = \sqrt{u^2 + v^2}$. The ECMWF wind speeds were interpolated in time using a linear interpolation procedure to fit the 15 minutes time steps of the in-situ data.

### *2.2. PV cell temperature prediction models*

Eight different models were tested to predict PV cell temperature. All models parameterize the physical relation between cell temperature, incoming irradiance and relevant meteorological parameters. The first tested model is the most commonly used standard approach, which does not include the wind cooling effect. The seven other tested models (Skoplaki 1, Skoplaki 2, Skoplaki 3, Koehl, Mattei 1, Mattei 2 and Kurtz) evaluate the PV module temperature as a function of solar irradiance, ambient temperature, wind speed and, in the case of Skoplaki 3, wind direction. In the following we give the details of the prediction models we tested.

**Standard approach**: The description of the so called NOCT-Standard-formula can be found in Markvart [9]. The cell temperature $T_c$ is calculated according to:

$$T_c = T_a + \frac{I}{I_{\mathrm{NOCT}}} \cdot (T_{NOCT} - T_{a,NOCT}) \quad (1)$$

$T_a$ is the ambient temperature, $I$ is the in-plane irradiance and $T_{NOCT}$ is the technology dependent nominal operating cell temperature, which is the cell temperature at irradiance $I_{\mathrm{NOCT}} = 800\ \mathrm{W}/m^2$, ambient temperature $T_{a,NOCT} = 20\ ^oC$ and wind speed 1 m/s. $T_{NOCT}$ depends on the PV technology and has a typical value of about 45 °C. Values for $T_{NOCT}$ for all investigated PV technologies are listed in table 1.

**Skoplaki 1 / Skoplaki 2 / Skoplaki 3**: Skoplaki et al. [5] suggest an advanced model to integrate wind data in the NOCT-Standard-formula (eq. (1)). This model considers - in addition to the ambient temperature $T_a$ and the in-plane irradiance $I$ - also wind speed $v$ and specific solar cell properties, such as efficiency $\eta$, temperature coefficient of maximal power $\beta$, transmittance of the cover system $\tau$ and absorption coefficient of the cells $\alpha$:

$$T_c = T_a + \frac{I}{I_{NOCT}} \cdot (T_{NOCT} - T_{a,NOCT}) \cdot \frac{h_{w,NOCT}}{h_w(v)} \cdot \left[1 - \frac{\eta_{STC}}{\tau \cdot \alpha}(1 - \beta_{STC} T_{STC})\right] \quad (2)$$

$\eta_{STC}$ and $\beta_{STC}$ are efficiency and temperature coefficient of maximal power under standard test conditions (STC): irradiance 1000 W/m², ambient temperature $T_{STC} = 25\ ^oC$ and air mass $AM = 1.5$. Values for $\eta_{STC}$ and $\beta_{STC}$ for the investigated PV technologies are listed in table 1. The value for $\tau \cdot \alpha$ can be usually assumed as 0.9 [5]. $h_w$ is the wind convection coefficient, which is typically a linear function of the wind velocity $v$. Skoplaki et al. [5] present two different parameterizations for $h_w$:

$$h_w = 8.91 + 2.00\ v_f \text{ (called here Skoplaki 1)} \quad (3)$$

$$h_w = 5.7 + 2.8\ v_w \text{ (called here Skoplaki 2)} \quad (4)$$

$v_w$ is the local wind speed close to the module, whereas $v_f$ is the wind speed measured 10 meters above the ground.

For the transformation between the two different wind speeds we used [10]:

$$v_w = 0.68\, v_f - 0.5 \tag{5}$$

$h_{w,NOCT}$ is the wind convection coefficient for wind speed at NOCT conditions, i.e. $v_w = 1\ m/s$.
Another parameterization for $h_w$ is suggested in Armstrong and Hurley [11] and Sharples and Charlesworth [12]:

$$h_w = 8.3 + 2.2\, v_w \tag{6}$$

for wind direction perpendicular to the module's surface and

$$h_w = 6.5 + 3.3\, v_w \tag{7}$$

for wind direction parallel to the module's surface.
We used relation (6) for wind directions perpendicular ($\pm$ 45°) to the module's surface and relation (7) for wind directions parallel ($\pm$ 45°) to the module's surface. The cell temperature calculated with eq. (2) and the parameterization for $h_w$ of Sharples is called here Skoplaki 3.

**Koehl:** Koehl et al. [6] used a simple empirical model, proposed by Faimann [13], to estimate the cell temperature $T_c$ as a function of in-plane irradiance $I$, ambient temperature $T_a$ and local wind speed near the modules $v_w$:

$$T_c = T_a + \frac{I}{U_0 + U_1 \cdot v_w} \tag{8}$$

The constants $U_0$ and $U_1$ are specified by Koehl et al. [6] for selected PV cell technologies and can be found in table 1.

**Mattei:** Mattei et al. [2] propose to model the PV cell temperature $T_c$ as:

$$T_c = \frac{U_{PV}(v)\, T_a + I \cdot [\tau \cdot \alpha - \eta_{STC}(1 - \beta_{STC}\, T_{STC})]}{U_{PV}(v) + \beta_{STC} \cdot \eta_{STC} \cdot I} \tag{9}$$

with in-plane irradiance $I$, ambient temperature $T_a$ and wind speed $v$.
The input parameters $\eta_{STC}$, $\beta_{STC}$ and $T_{STC}$ are the same as in the Skoplaki model (eq. (2) and table 1). Mattei et al. [2] used $\tau \cdot \alpha = 0.81$.
$U_{PV}(v)$ is the heat exchange coefficient for the total surface of the module. It was calculated by Mattei et al. [2]. They report two different parameterizations:

$$U_{PV}(v_w) = 26.6 + 2.3\, v_w \text{ (called here Mattei 1)} \tag{10}$$

$$U_{PV}(v_w) = 24.1 + 2.9\, v_w \text{ (called here Mattei 2)} \tag{11}$$

$v_w$ is the local wind speed close to the module.

**Kurtz:** Kurtz et al. [7] used the following relation to calculate the module temperature $T_c$:

$$T_c = T_a + I \cdot e^{-3.473 - 0.0594 \cdot v_w} \tag{12}$$

Here $T_a$ is the ambient temperature, $I$ is the in-plane irradiance and $v_w$ is the local wind speed close to the module. The formula of Kurtz et al. [7] does not distinguish between different PV technologies.

### 2.3. Statistical method

In order to compare and study the different theoretical models, we investigated 15 minutes, hourly and daily averaged data. We compared the measured cell temperature $T_{meas}$ and modelled cell temperature $T_c$ for each time interval, each module technology and each model. A perfect model calculates the cell temperature exactly ($T_c = T_{meas}$) and thus, the relation between $T_{meas}$ and $T_c$ is linear. Hence, we calculated the coefficient of determination ($R^2$) and the root mean squared error (RMSE) of this comparison. We considered both $R^2$ and RMSE to measure the linearity of the investigated phenomenon and the associated error to obtain a quantitative indication of the model performance.

## 3. Results and Discussion

### 3.1. In-situ wind data

The values of $R^2$ and RMSE for the in-situ wind data analysis (three different time intervals, five different technologies and eight different models) are listed in table 2 (left columns). The results are visualized in figure 1 (a, c, e), where the scatterplots of $R^2$ and RMSE values for all the models (grouped with different symbols) and all the investigated PV technologies (grouped with different colours) are shown. The results presented in figure 1 and table 2 must be interpreted as follows: the best model is the one that minimizes RMSE and maximizes $R^2$.

For all four silicon PV technologies, the models which include in-situ wind data give more accurate results than the standard approach, in which wind is not considered (table 1, figure 2). We can deduce that for the polycrystalline silicon technology (black, figure 1) the models Mattei 1 and 2 [2] perform better than the others. For microcrystalline silicon (red, figure 1) and monocrystalline silicon (green, figure 1) the Skoplaki 2 model [5] performs slightly better than Mattei 1 which continues to give good values. For amorphous silicon (magenta, figure 1) the Koehl model [6] performs much better than the others. However, for CdTe (blue, figure 1) the standard model [4, 9] and the approach of Kurtz [7] give the best results, probably because those PV modules have a higher thermal inertia than the silicon PV technologies. From this analysis it can be clearly seen that it is not possible to provide a unique indication of the most suitable model to calculate the PV cell temperature. However, it must be highlighted how crucial it is to include wind parameterization to estimate the PV module temperature.

Considering the different time intervals, $R^2$ values are lower for 15 minutes data and higher for daily averages, vice versa RMSE is lower when daily averages are considered. Averaging on longer time scales tends to stabilize the results and to moderate the short-term variability.

### 3.2. ECMWF wind data

We repeated our analysis using in-situ temperature and irradiance data combined with wind data obtained from the ECMWF model. The results are shown in table 2 (right columns) and figure 1 (b, d, f). For this study we did not include the model Skoplaki 3, which requires estimates of the wind direction. Wind directions cannot be obtained accurately from the interpolation of 6 hourly ECMWF wind fields at our test site, since they can change very rapidly in mountainous regions. Compared to the analysis carried out with in-situ wind data, we observe lower $R^2$ and higher RMSE. However, models including ECMWF wind speed give in general significantly better results than the standard formula. Moreover, the model performance is different compared to the in-situ wind data analysis: all technologies are well modelled by Mattei 1 and Mattei 2 with Mattei 1 performing slightly better than Mattei 2. Furthermore, the behaviour

Table 2. Performance of different approaches to estimate the PV cell temperature as a function of in-situ and ECMWF wind speed/direction measurements and/or irradiance and ambient temperature from March 2011 to February 2012 from our multi-technology photovoltaic test-facility at the Airport Bolzano Dolomiti (ABD). Reported are the coefficient of determination ($R^2$) and the root mean squared error (RMSE) for polycrystalline silicon (p-Si), microcrystalline silicon (µc-Si), cadmium telluride (CdTe), amorphous silicon (a-Si) and monocrystalline silicon (m-Si). The Standard formula does not include wind data, while the other listed models consider wind measurements. The model Skoplaki 3 is not included in the ECMWF data analysis, since it uses wind direction, which cannot be interpolated meaningfully from 6 hourly ECMWF wind fields for the fast changing wind directions in alpine regions. For all PV technologies except CdTe and for both in-situ and ECMWF wind data, the models that include wind data perform significantly better than the standard approach.

| | | **in-situ wind data** | | | | | | **ECMWF wind data** | | | | | |
|---|---|---|---|---|---|---|---|---|---|---|---|---|---|
| | | 15 minutes | | hourly mean | | daily mean | | 15 minutes | | hourly mean | | daily mean | |
| Model | Technology | $R^2$ | RMSE (K) | $R^2$ | RMSE (K) | $R^2$ | RMSE (K) | $R^2$ | RMSE (K) | $R^2$ | RMSE (K) | $R^2$ | RMSE (K) |
| Standard | p-Si | 0.80 | 7.5 | 0.80 | 7.3 | 0.79 | 7.0 | 0.80 | 7.5 | 0.80 | 7.3 | 0.79 | 7.0 |
| Standard | µc-Si | 0.86 | 6.1 | 0.86 | 5.9 | 0.86 | 5.4 | 0.86 | 6.1 | 0.86 | 5.9 | 0.86 | 5.4 |
| Standard | CdTe | 0.94 | 3.9 | 0.96 | 3.2 | 0.97 | 2.5 | 0.94 | 3.9 | 0.96 | 3.2 | 0.97 | 2.5 |
| Standard | a-Si | 0.81 | 7.2 | 0.82 | 6.9 | 0.82 | 6.5 | 0.81 | 7.2 | 0.82 | 6.9 | 0.82 | 6.5 |
| Standard | mo-Si | 0.76 | 8.0 | 0.77 | 7.8 | 0.76 | 7.3 | 0.76 | 8.0 | 0.77 | 7.8 | 0.76 | 7.3 |
| Skoplaki 1 | p-Si | 0.95 | 3.3 | 0.96 | 3.0 | 0.96 | 2.8 | 0.93 | 4.0 | 0.94 | 3.7 | 0.94 | 3.4 |
| Skoplaki 1 | µc-Si | 0.96 | 2.9 | 0.97 | 2.5 | 0.97 | 2.2 | 0.94 | 3.7 | 0.94 | 3.5 | 0.95 | 3.0 |
| Skoplaki 1 | CdTe | 0.91 | 4.4 | 0.93 | 3.9 | 0.94 | 3.4 | 0.90 | 4.8 | 0.91 | 4.3 | 0.92 | 3.8 |
| Skoplaki 1 | a-Si | 0.92 | 4.3 | 0.93 | 3.9 | 0.93 | 3.7 | 0.89 | 5.1 | 0.90 | 4.8 | 0.91 | 4.3 |
| Skoplaki 1 | mo-Si | 0.95 | 3.1 | 0.96 | 2.7 | 0.97 | 2.4 | 0.92 | 4.0 | 0.93 | 3.8 | 0.94 | 3.1 |
| Skoplaki 2 | p-Si | 0.95 | 3.3 | 0.96 | 2.8 | 0.97 | 2.4 | 0.92 | 4.1 | 0.93 | 3.9 | 0.93 | 3.5 |
| Skoplaki 2 | µc-Si | 0.96 | 2.7 | 0.98 | 2.1 | 0.98 | 1.6 | 0.93 | 3.8 | 0.94 | 3.6 | 0.95 | 3.1 |
| Skoplaki 2 | CdTe | 0.87 | 5.2 | 0.89 | 4.7 | 0.90 | 4.1 | 0.88 | 5.2 | 0.89 | 4.8 | 0.90 | 4.3 |
| Skoplaki 2 | a-Si | 0.92 | 4.1 | 0.94 | 3.6 | 0.95 | 3.1 | 0.89 | 5.1 | 0.90 | 4.8 | 0.90 | 4.4 |
| Skoplaki 2 | mo-Si | 0.96 | 2.8 | 0.97 | 2.3 | 0.98 | 1.9 | 0.92 | 4.1 | 0.92 | 3.9 | 0.94 | 3.3 |
| Skoplaki 3 | p-Si | 0.94 | 3.6 | 0.95 | 3.3 | 0.95 | 3.1 | - | - | - | - | - | - |
| Skoplaki 3 | µc-Si | 0.95 | 3.2 | 0.96 | 2.9 | 0.96 | 2.6 | - | - | - | - | - | - |
| Skoplaki 3 | CdTe | 0.92 | 4.2 | 0.94 | 3.7 | 0.95 | 3.1 | - | - | - | - | - | - |
| Skoplaki 3 | a-Si | 0.91 | 4.6 | 0.92 | 4.3 | 0.92 | 4.0 | - | - | - | - | - | - |
| Skoplaki 3 | mo-Si | 0.94 | 3.4 | 0.95 | 3.1 | 0.96 | 2.7 | - | - | - | - | - | - |
| Koehl | p-Si | 0.95 | 3.3 | 0.96 | 3.0 | 0.96 | 2.8 | 0.93 | 3.8 | 0.94 | 3.6 | 0.94 | 3.3 |
| Koehl | µc-Si | 0.95 | 3.3 | 0.96 | 3.0 | 0.96 | 2.7 | 0.93 | 4.0 | 0.94 | 3.7 | 0.94 | 3.2 |
| Koehl | CdTe | 0.94 | 4.1 | 0.96 | 3.3 | 0.96 | 2.9 | 0.91 | 4.8 | 0.93 | 4.3 | 0.94 | 3.8 |
| Koehl | a-Si | 0.96 | 2.8 | 0.98 | 2.2 | 0.98 | 1.7 | 0.93 | 4.0 | 0.93 | 3.7 | 0.95 | 3.1 |
| Koehl | mo-Si | 0.91 | 4.4 | 0.92 | 4.2 | 0.92 | 3.9 | 0.88 | 5.0 | 0.89 | 4.8 | 0.90 | 4.3 |
| Mattei 1 | p-Si | 0.98 | 2.2 | 0.98 | 1.9 | 0.99 | 1.4 | 0.97 | 2.5 | 0.98 | 2.2 | 0.98 | 1.7 |
| Mattei 1 | µc-Si | 0.96 | 2.9 | 0.97 | 2.6 | 0.98 | 2.1 | 0.95 | 3.2 | 0.96 | 2.9 | 0.97 | 2.3 |
| Mattei 1 | CdTe | 0.85 | 5.5 | 0.87 | 5.1 | 0.88 | 4.7 | 0.85 | 5.6 | 0.86 | 5.3 | 0.87 | 4.8 |
| Mattei 1 | a-Si | 0.95 | 3.1 | 0.96 | 2.8 | 0.97 | 2.2 | 0.95 | 3.4 | 0.96 | 3.1 | 0.97 | 2.4 |
| Mattei 1 | mo-Si | 0.96 | 2.9 | 0.97 | 2.6 | 0.98 | 1.9 | 0.95 | 3.2 | 0.95 | 2.9 | 0.97 | 2.1 |
| Mattei 2 | p-Si | 0.97 | 2.5 | 0.98 | 2.2 | 0.98 | 1.8 | 0.96 | 2.9 | 0.97 | 2.6 | 0.98 | 2.1 |
| Mattei 2 | µc-Si | 0.95 | 3.3 | 0.96 | 3.0 | 0.96 | 2.7 | 0.94 | 3.7 | 0.94 | 3.4 | 0.96 | 2.9 |
| Mattei 2 | CdTe | 0.90 | 4.7 | 0.91 | 4.3 | 0.92 | 3.8 | 0.89 | 4.9 | 0.90 | 4.6 | 0.91 | 4.1 |
| Mattei 2 | a-Si | 0.94 | 3.6 | 0.95 | 3.3 | 0.96 | 2.9 | 0.93 | 4.0 | 0.94 | 3.6 | 0.95 | 3.1 |
| Mattei 2 | mo-Si | 0.95 | 3.0 | 0.96 | 2.7 | 0.97 | 2.2 | 0.94 | 3.5 | 0.95 | 3.2 | 0.96 | 2.5 |
| Kurtz | p-Si | 0.90 | 4.9 | 0.91 | 4.7 | 0.90 | 4.5 | 0.90 | 5.0 | 0.90 | 4.8 | 0.90 | 4.5 |
| Kurtz | µc-Si | 0.90 | 5.0 | 0.90 | 4.8 | 0.91 | 4.4 | 0.89 | 5.2 | 0.90 | 4.9 | 0.90 | 4.5 |
| Kurtz | CdTe | 0.95 | 3.6 | 0.96 | 3.0 | 0.97 | 2.3 | 0.94 | 3.8 | 0.96 | 3.3 | 0.97 | 2.6 |
| Kurtz | a-Si | 0.91 | 4.6 | 0.92 | 4.3 | 0.92 | 4.0 | 0.90 | 4.8 | 0.91 | 4.5 | 0.92 | 4.0 |
| Kurtz | mo-Si | 0.84 | 6.1 | 0.85 | 5.9 | 0.85 | 5.6 | 0.84 | 6.3 | 0.84 | 6.1 | 0.85 | 5.6 |

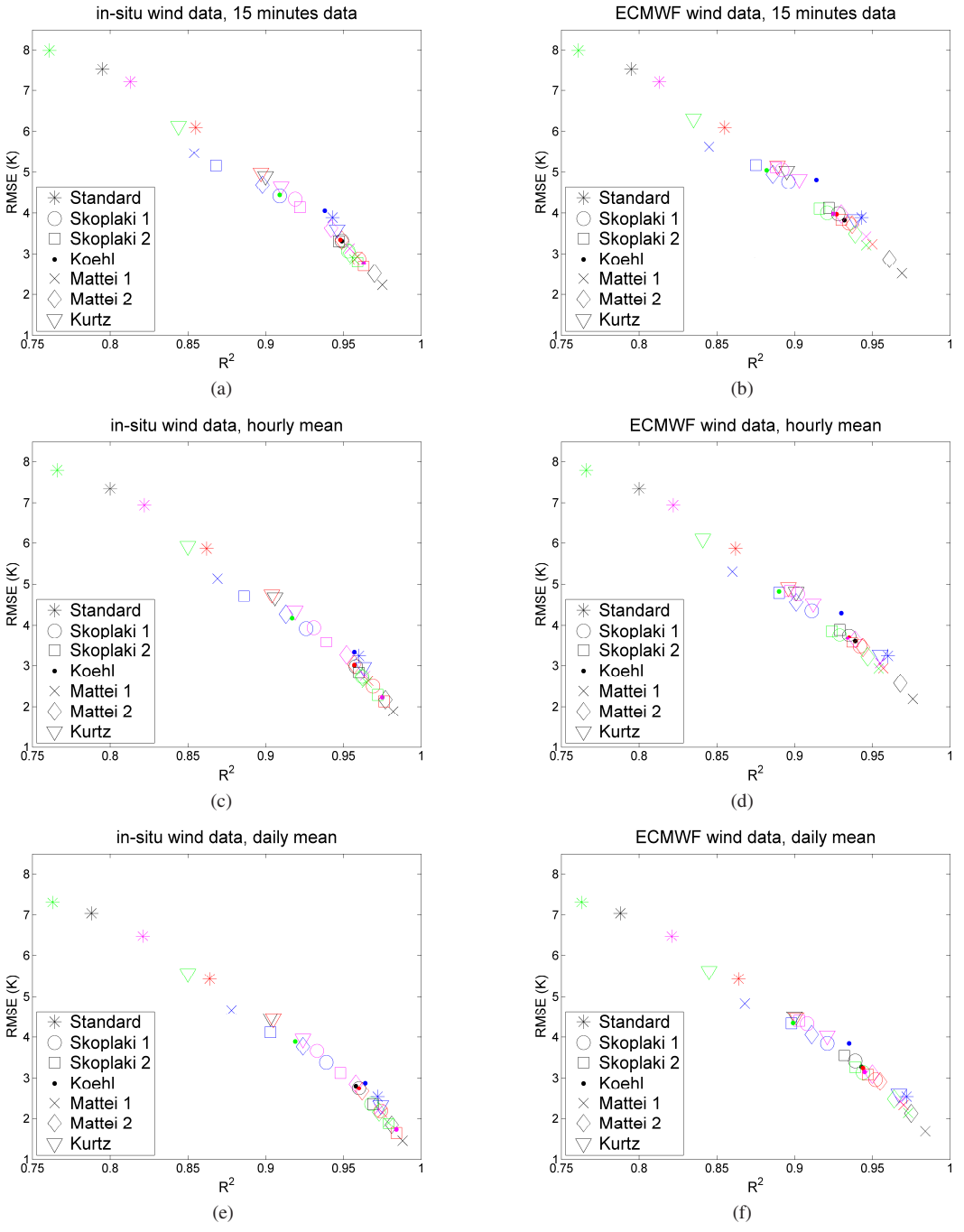


Fig. 1. Scatter plots of $R^2$ and RMSE (K) obtained comparing the linear relation between measured and modelled PV module temperature. The colours refer to different technologies: polycrystalline silicon (black), microcrystalline silicon (red), monocrystalline silicon (green), amorphous silicon (magenta) and CdTe (blue). The shapes describe the used model and are explained in the legend. For the plots on the left side the wind data are obtained from in-situ instruments, for the plots on the right side the wind data are obtained from the ECMWF model

of the CdTe technology is confirmed: the standard model (which does not include wind) and the Kurtz model are the most representative.

The observed differences between the first (in-situ wind data) and second (NWP wind data) analysis can be ascribed directly by the wind data sources: in the first case we used wind data from the anemometer present in-situ which measures small scale wind motion and variability; in the second case the data were obtained by the ECMWF model and refer to the nearest model grid point that is supposed to be representative for a larger area. The up-scaling effect passing from the in-situ measurement to the grid model data is particularly significant in complex orographic regions and in mountain areas, like the one of interest for this study. However, our comparison between the use of in-situ and ECMWF model wind data shows two important results: i) the inclusion of wind in the modules temperature estimation is significant; ii) wind data from NWP model allow an estimation of the module temperature with an error of the same order of magnitude as the in-situ data analysis.

## 4. Conclusions

In this study we tested several existing models to evaluate the PV module temperature as a function of solar irradiance, ambient temperature and wind. We used data from a large PV power plant from the city of Bolzano (Italy) located at the bottom of an alpine valley. This PV power plant consists of different PV technologies and is equipped with several instruments to monitor solar radiation, wind speed and direction, ambient and PV cell temperatures [8].

We found that, using the most common approaches to evaluate the PV module temperature, the inclusion of wind cooling effects plays a fundamental role for a better estimation. We observed that for in-situ wind data, the Mattei 1 formulation [2] is suitable to describe the behaviour of the polycrystalline, microcrystalline and monocrystalline silicon technologies, although for the last two the Skoplaki 2 model [5] performs slightly better. For amorphous silicon the Koehl method [6] is the most accurate with the highest $R^2$ and the lowest RMSE. In contrast, for the CdTe modules the approach of Kurtz et al. [7] as well as the standard formula [4, 9] performs better than the others. Considering numerical weather prediction (NWP) data the Mattei 1 and Mattei 2 approaches [2] are the most promising for all silicon technologies, but for CdTe the Kurtz and the standard methods continue to perform best.

Concluding, the results can be summarized as:

1) The role of wind is relevant for the estimation of the PV module temperature: for most technologies, models which include wind data have significantly higher values of $R^2$ and lower RMSE compared to the standard approach.
2) It is not possible to select a general approach to include wind in the estimation of the module temperature, since the model performances vary from technology to technology. Our results provide an indication of the model performances for the five technologies which were tested in our study.
3) Wind data from the European Centre for Medium range Weather Forecast (ECMWF) model can be used in locations in which in-situ wind data are missing. Although the values of $R^2$ and RMSE are slightly worse than for the calculations with in-situ wind data, they still give much better results than the standard formula.
4) Following the approaches we proposed, it is possible to obtain power production estimations for PV power plants at regional scale using wind data from NWP models. This can be of importance for stakeholders who have to plan energy policies and energy management programs.

The validity of the results of this study is not general and it must be limited to the region investigated. We are currently collecting data from other locations in order to continue the analysis and to generalize the results obtained.

## Acknowledgements

This study was carried out in the framework of the PV-Alps INTERREG project in which the energy potential of different photovoltaic technologies is analysed for alpine regions (www.pvalps.eurac.edu). The research was financed through the INTERREG program IV Italy - Swiss by the European Funds for Regional Development (EFRE). The data monitoring at the ABD airport was funded through ERDF project PV-Initiative. We thank the ECMWF for providing the wind data for this study.

## References

[1] Deutsche Gesellschaft für Sonnenenergie. *Photovoltaische Anlagen* (in German). 4th edition. Chap. 3. Berlin: Berlin Brandenburg e.V.; 2010.

[2] Mattei M, Notton G, Cristofari G, Muselli M, Poggi P. Calculation of the polycrystalline PV module temperature using a simple method of energy balance. *Renew Energ* 2006; **31**: p. 553-567.

[3] King DL, Boyson WE, Kratochvil JA. Analysis of factors influencing the annual energy production of photovoltaic systems. In: *Conference Record of the Twenty-Ninth IEEE Photovoltaic Specialists Conference*, 2002: p. 1356-1361.

[4] Skoplaki E, Palyvos JA. Operating temperature of photovoltaic modules: A survey of pertinent correlations. *Renew Energ* 2009*;* **34**: p. 23-29.

[5] Skoplaki E, Boudouvis AG, Palyvos JA. A simple correlation for the operating temperature of photovoltaic modules of arbitrary mounting. *Sol Energ Mat Sol C* 2008; **92**: p. 1393-1402.

[6] Koehl M, Heck M, Wiesmeier S, Wirth J. Modeling of the nominal operating cell temperature based on outdoor weathering. *Sol Energ Mat Sol C* 2011; **95**: p. 1638-1646.

[7] Kurtz S, Whitfield K, Miller D, Joyce J, Wohlgemuth J, Kempe M, et al. Evaluation of high-temperature exposure of rack-mounted photovoltaic modules. In: *34th IEEE Photovoltaic Specialists Conference (PVSC)*, 2009: p. 2399-2404.

[8] Belluardo G, Pichler M, Moser D, Nikolaeva-Dimitrova M. One-year comparison of different thin film technologies at Bolzano Airport Test Installation. In: Méndez-Vilas A, editor. *Fuelling the Future: Advances in Science and Technologies for Energy Generation, Transmission and Storage*, Boca Raton: Brown Walker Press; 2012, p. 229-234.

[9] Markvart T (editor). *Solar electricity*. 2nd edition. Chichester: Wiley; 2000.

[10] Loveday DL, Taki AH. Convective heat transfer coefficients at a plane surface on a full-scale building facade. *Int J Heat Mass Trans* 1996; **39** (8): p. 1729 – 1742.

[11] Armstrong S, Hurley WG. A thermal model for photovoltaic panels under varying atmospheric conditions. *Appl Therm Eng* 2010; **30**: p. 1488-1495.

[12] Sharples S, Charlesworth PS. Full-scale measurements of wind-induced convective heat transfer from a roof-mounted flat plate solar collector. *Sol Energy* 1998; **62**: p. 69-77.

[13] Faimann D. Assessing the Outdoor Operating Temperature of Photovoltaic Modules. *Prog Photovolt Res Appl* 2008, **16**: p. 307–315.